

## Article

# Mechanism and Evolution of Soil Organic Carbon Coupling with Rocky Desertification in South China Karst

Xingfu Wang <sup>1,†</sup>, Xianfei Huang <sup>1,†</sup> , Kangning Xiong <sup>1,\*</sup>, Jiwei Hu <sup>1</sup>, Zhenming Zhang <sup>2</sup> and Jiachun Zhang <sup>3</sup>

<sup>1</sup> State Engineering Technology Institute for Karst Desertification Control, School of Karst Science, Guizhou Normal University, Guiyang 550001, China; wang88xingfu@163.com (X.W.); hxfswjs@gznu.edu.cn (X.H.); jwhu@gznu.edu.cn (J.H.)

<sup>2</sup> Institute of Biology, Guizhou Academy of Sciences, Guiyang 550001, China; zhangzm@gzu.edu.cn

<sup>3</sup> Guizhou Botanical Garden, Guiyang 550001, China; zhangjiachun198806@163.com

\* Correspondence: xiongkn@gznu.edu.cn

† These authors contributed equally to this work.

**Abstract:** To study the spatial distribution characteristics of soil organic carbon (SOC) coupled with rocky desertification, 1212 soil samples from 152 soil profiles were sampled from different karst landforms, including karst low hills/virgin forest (KLH) in Libo County, a karst peak-cluster depression (KPCD) in Xingyi County, a karst canyon (KC) in Guanling County, a karst plateau basin (KPB) in Puding County and a karst trough valley (KTV) in Yinjiang County. The spatial distribution characteristics of the responses of SOC, SOC density (SOCD), rocky desertification and soil bulk density (SBD) to different influencing factors were analyzed. The relationships among SOC, SOCD, rocky desertification and SBD were analyzed using Pearson correlation analysis. The SOC storage capacity was characterized by using SOCD, and then the SOC storage capacity in different evolution stages of karst landforms was assessed. The SOC contents of KLH, KPCD, KC, KPB and KTV ranged from 6.16 to 38.20 g·kg<sup>-1</sup>, 7.42 to 27.08 g·kg<sup>-1</sup>, 6.28 to 35.17 g·kg<sup>-1</sup>, 4.62 to 23.79 g·kg<sup>-1</sup> and 5.24 to 37.85 g·kg<sup>-1</sup>, respectively, and their average SOCD values (0–100 cm) were 7.37, 10.79, 7.06, 8.51 and 7.84 kg·m<sup>-2</sup>, respectively. The karst landforms as ordered by SOC storage capacity were KPCD > KPB > KLH > KTV > KC. The SOC content was negatively correlated with the SBD; light rocky desertification may lead to SOC accumulation. The rocky desertification degree and SBD were closely associated with slope position and gradient. Rocky desertification first increased, then decreased from mountain foot to summit, and increased with increasing slope gradient. However, the SBD decreased from mountain foot to summit and with increasing slope gradient. The SOC contents on the northern aspect of the mountains were generally higher than the other aspects. In summary, rock outcrops controlled the SOC contents in the studied regions. The slope position, gradient and aspect influenced the composition and distribution of vegetation, which influenced the evolution of rocky desertification. Therefore, these factors indirectly affected the SOC content. Additionally, the SOCD decreased with increasing rocky desertification. During the different evolution stages of karst landforms, the SOC storage capacity first decreases, then increases.

**Keywords:** soil organic carbon; rocky desertification process; vegetation; spatial heterogeneity; response mechanism; different karst landforms



**Citation:** Wang, X.; Huang, X.; Xiong, K.; Hu, J.; Zhang, Z.; Zhang, J. Mechanism and Evolution of Soil Organic Carbon Coupling with Rocky Desertification in South China Karst. *Forests* **2022**, *13*, 28. <https://doi.org/10.3390/f13010028>

Academic Editor: Choonsig Kim

Received: 16 November 2021

Accepted: 22 December 2021

Published: 27 December 2021

**Publisher's Note:** MDPI stays neutral with regard to jurisdictional claims in published maps and institutional affiliations.



**Copyright:** © 2021 by the authors. Licensee MDPI, Basel, Switzerland. This article is an open access article distributed under the terms and conditions of the Creative Commons Attribution (CC BY) license (<https://creativecommons.org/licenses/by/4.0/>).

## 1. Introduction

Soil is an open system of matter and energy in nature, and accumulates matter and energy for conversion into other forms. Soil is a key component of the Earth system controlling processes involved in mass flow, energy flow and biogeochemical cycles [1,2]. Soil is a loose layer covering the Earth's land surface in which plants grow, and is an important reservoir of soil organic carbon (SOC) [3,4]. SOC is an important basis for soil fertility, and plays a key role in improving soil quality and promoting agricultural output [5]. Soil ecosystems provide nutrients for plant growth, support biological processes

and impact the composition of the atmosphere, e.g., they adjust the balance of moisture, heat and carbon dioxide. Therefore, soil quality is key to the sustainable development of ecological environments [6,7]. Previous studies have shown that the global SOC reserve in the 0–100 cm soil layer is approximately 1460 Pg, which is three times and two times greater than the SOC reserve in vegetation and the atmosphere, respectively [8–10]. The SOC reservoir is a key part of the terrestrial carbon pool, and a small change in SOC may lead to a huge change in atmospheric CO<sub>2</sub> concentration, which is associated with global warming [11]. The SOC reservoir has a direct impact on terrestrial SOC storage, which influences the global carbon balance [12–14]. The SOC is not permanently fixed in soils, and is a dynamic process of outputs and inputs [15,16]. Karst landforms are unique ecosystems that differ from non-karst areas and are characterized by low stability, poor self-regulation and low environmental capacity. The spatial distribution of SOC in karst areas is highly heterogeneous [17,18]. The spatial heterogeneity of SOC and the ecological environment in karst areas is much greater than in non-karst areas [19]. The problem of global carbon loss remains unresolved, and many scholars are focusing on SOC in karst regions for answers [20,21]. Research on SOC in karst areas has become a hot topic worldwide.

The ecological environment in karst areas is complex. Many factors influence the spatial distribution and storage of SOC in karst areas, including lithology, slope gradient, slope aspect, slope position, rock exposure and vegetation [13,22]. The slope gradient has a significant effect on changes in SOC content in the topsoil layer (0–20 cm) [23]. Zhang et al. found that slope gradient and slope aspect were important factors in afforestation that drove soil carbon sequestration and reduced soil erosion [24]. Liu et al. reported that land use played a key role in affecting variations in SOC in dry valleys in southwestern China [25]. Zhang et al. found that paddy fields improved SOC accumulation in karst basins [14]. The reclamation of farmland as forest is a key measure in the remediation of karst rocky desertification in Southwest China; it changes the local land use, which affects the local SOC spatial distribution and storage [19]. Many scholars have investigated the spatial distribution characteristics and reserves of SOC in karst areas in southern China. For example, Zhang et al. investigated the SOC in the Houzhai karst basin of Guizhou Province from 1980–2015; their results showed that the SOC density in the topsoil layer of 0–20 cm increased from 4.91 to 5.13 kg·m<sup>-2</sup>, the SOC content was between 21.91 and 25.07 g·kg<sup>-1</sup>, and the SOC storage was between 368.27 × 10<sup>3</sup> and 385.09 × 10<sup>3</sup> t [14,22]. These results were similar to Huang et al., who stated that the average SOC content, density and total storage at a soil depth of 20 cm in a small karst watershed were 25.07 g·kg<sup>-1</sup>, 4.27 kg·m<sup>-2</sup> and 2.65 × 10<sup>8</sup> kg, respectively [19,26]. The SOC storage in the 0–20 cm soil layer accounted for 49.2% of the SOC storage in the 0–100 cm soil layer (5.39 × 10<sup>8</sup> kg) [13,26]. Huang et al. predicted that SOC storage in the 0–20 cm and 0–100 cm soil layers would increase to 3.37 × 10<sup>13</sup> g and 6.29 × 10<sup>13</sup> g by 2050 with the implementation of a rocky desertification control project (returning farmland to forests and grass) in Guizhou Province [19]. In general, the SOC gradually decreased with increasing soil depth in the 0–100 cm soil layer. Humans can easily disturb the SOC in the upper 0–50 cm soil layer, and changes to the SOC fit a linear model. However, little difference was found in SOC in the 50–100 cm subsoil layer [20]. There were some discrepancies in SOC content and storage among the different karst landforms. Wang et al. found that the SOC content in the 0–20 cm soil layer ranged from 20.29 to 31.02 g·kg<sup>-1</sup> in different karst landforms, which is a highly variable level [15]. In profile of 100 cm, the SOC densities (SOCD) in a karst basin, a karst trough valley and a karst area in southwestern China were 8.7 kg·m<sup>-2</sup> [26], 10.6 kg·m<sup>-2</sup> [27] and 5.62 kg·m<sup>-2</sup> [28], respectively. Wang et al. showed that the SOCD in the 0–40 cm soil depth was between 1.08 and 7.32 kg·m<sup>-2</sup> under different rocky desertification degrees, with the magnitude of this range reaching 6.24 kg·m<sup>-2</sup> [21].

Many scholars have examined the spatial distribution characteristics of the content, density, and storage of SOC and the controlling factors in karst areas. However, there are few reports on the SOC response to different factors coupled with rocky desertification stages on different karst landforms. Therefore, the present study investigated the SOC

spatial distribution response to different factors (e.g., slope gradient, slope aspect, slope position, vegetation, lithology and climate) with rocky desertification characteristics. The results improve our understanding of the regularity of the spatial distribution and storage capacity of SOC in karst rocky desertification areas, and provide a reference for carbon sink management and environmental protection in these areas.

## 2. Materials and Methods

### 2.1. Study Region

The study areas were locations in Guizhou Province in Southwest China with the geographic coordinates  $103^{\circ}36'–109^{\circ}35'$  E and  $24^{\circ}37'–29^{\circ}13'$  N, including Libo County, Xingyi County, Guanling County, Puding County and Yinjiang County. The research region is located in the slope belt of the transition zone between the Sichuan Basin (Sichuan Province), the Yun-Gui Plateau (Yunnan Province and Guizhou Province) and the Hunan Hills (Hunan Province). The elevation in the region ranges from 147.7 m to 2900.6 m, and the area features high mountains, deep valleys and steep slopes. The terrain in the western part is higher in elevation than the eastern part, and the main landform types include karst plateaus, karst mountains, karst hills and karst basins. Mountains and hills account for 92.5% of the total area. The karst area accounts for 61.56% of the terrestrial area, and the rocky desertification area accounts for 34.59%. This area is in the subtropical region, features a humid monsoon climate, and is affected by the quasi-stationary Guiyang–Kunming front. The average annual temperature is between  $13^{\circ}\text{C}$  and  $16^{\circ}\text{C}$ , and the average annual rainfall is between 1150 mm and 1250 mm. The rainy season and the warm season coincide, which may promote further rocky desertification. Based on the findings of the survey and statistical analysis, tree species primarily include *Juglans regia* L., *Cyclobalanopsis glauca* (Thunb.) Oerst. and *Pinus massoniana* Lamb., shrub species primarily include *Rose roxburghii* and *Pyracantha fortuneana* (Maxim.) Li, and grass species primarily include *Setaria viridis* (L.) Beauv. and *Eleusine indica* (L.) Gaertn.

### 2.2. Research Design

To research the spatial distribution characteristics of the responses of SOC content and storage capacity to the different geographical factors associated with rocky desertification processes on different karst landforms, soil samples were taken from a virgin forest region in Libo, a peak cluster depression in Xingyi, a canyon in Guanling, a basin in Puding and a trough valley in Yinjiang. These regions represent karst low hills (KLH), karst peak-cluster depression (KPCD), karst canyon (KC), karst plateau basin (KPB) and karst trough valley (KTV), respectively. The slope position of the mountain was divided into four parts: flat ground (zone I), lower part of the mountain (zone II), middle part of the mountain (zone III) and upper part of the mountain (zone IV). The slope gradient was classified as A type (slope  $< 20^{\circ}$ ), B type ( $20 \leq \text{slope} < 40^{\circ}$ ), C type ( $40 \leq \text{slope} < 60^{\circ}$ ) and D type (slope  $\geq 60^{\circ}$ ). The sampling points were set on the mountain surface from the mountain bottom to the mountain top. Each sampling profile was dug to a depth of 100 cm where possible, and the soil profile was divided into twelve layers: 0–5 cm, 5–10 cm, 10–15 cm, 15–20 cm, 20–30 cm, 30–40 cm, 40–50 cm, 50–60 cm, 60–70 cm, 70–80 cm, 80–90 cm and 90–100 cm.

According to the model of exchanging space for time, the rocky desertification degree was divided into five levels by determining the percentage of rock outcrops [16,21,29]. This classification reflects the dynamic characteristics of the karst rocky desertification process. Higher percentages of rock outcrops indicate more severe rocky desertification (Table 1).

The process of karst landform evolution is divided into four main stages: infancy (stage I), youth (stage II), middle age (stage III) and older (stage IV). The main karst features in stage I include stone teeth, lapie and dolines. The main karst features in stage II include blind valleys, dry valleys, shafts and reculee. The main karst features in stage III include peak forests, peak clusters and karst depressions. The main karst features in stage IV include karst plains, karst hills and solitary peaks. The KPB and KTV belonged to stage I in the present study, KC belonged to stage II, KPCD belonged to stage III, and KLH belonged

to stage IV. During the evolution process, the rocky desertification degree increased quickly from stage I to stage II, decreased sharply from stage II to stage III, and finally increased slowly from stage III to stage IV.

**Table 1.** Rocky desertification classes in karst areas.

	Class				
	1	2	3	4	5
Percentage of rock outcrops (%)	$0 \leq X < 20$	$20 \leq X < 40$	$40 \leq X < 60$	$60 \leq X < 80$	$80 \leq X \leq 100$
Type of ground material composition	Soil	Soil-based	Soil and stone	Stone-based	Stone
Rocky desertification degree	Low	Low to moderate	Moderate	Medium to high	High

### 2.3. Soil Sampling and Field Investigation

The sampling sites were set by a random method according to the statistical theory proposed by Fisher in 1956 [30]. This is a simple, convenient and highly feasible method. In the sampling process, the random samples can reflect the general conditions of study area at a high level, and the chance of any sampling point being sampled is equal [31,32]. The random sampling method is appropriate for use in karst areas because of the high heterogeneity of the environmental characteristics.

Soil thickness was less than 100 cm at many sampling points in the field, which resulted in the actual sample number being smaller than the planned sample number. A total of 1212 soil samples were collected from 152 points in the studied regions. Among these soil samples, 155 soil samples were collected from 25 soil profiles in KLH, 227 soil samples were collected from 22 soil profiles in KPCD, 167 soil samples were collected from 25 soil profiles in KC, 479 soil samples were collected from 53 soil profiles in KPB, and 184 soil samples were collected from 27 soil profiles in KTV. Other information, such as the slope position, slope gradient, slope aspect, vegetation, soil bulk density (SBD), rock outcrops, and lithology was recorded simultaneously for each of the sampling points. The SBD was tested using the cutting ring method [22]. The rock outcrops around the soil sampling points were evaluated using the line-transect method with a line 10 m in length [15,20]. Soil samples were stored in sealed plastic bags and numbered; the weight of each soil sample was approximately 1 kg. All soil sample bags were taken back to the laboratory, air-dried, ground, weighed, sieved to remove the gravel fraction (>2 mm), and prepared as required for laboratory analysis [18,33]. Rainfall information for the different counties was obtained from the Resource and Environment Science and Data Center of the Chinese Academy of Sciences.

### 2.4. SOC Determination and Statistical Analysis

#### 2.4.1. The Calculation of SBD and SOC

The SBD was calculated using the following formula [15]:

$$SBD = \frac{M_2 - M_1}{V} \quad (1)$$

where  $M_1$  is the weight of the cutting ring (g),  $M_2$  is the weight of the cutting ring with dry soil (g), and  $V$  is the volume of the cutting ring ( $\text{cm}^3$ )

The SOCD was calculated based on the SOC content using the following formulas [34–36]:

$$SOCD = \sum_{m=1}^{n+1} \frac{SOC_m \times SBD_m \times H_m \times (1 - \theta_m) \times (1 - A_r)}{1 - M_m} \quad (2)$$

where  $n$  is the number of soil samples collected from the sampling site,  $SOC_m$  is the SOC concentration of the  $m$  layer ( $\text{g} \cdot \text{kg}^{-1}$ ),  $SBD_m$  is the soil bulk density ( $\text{g} \cdot \text{cm}^{-3}$ ) of the  $m$  layer,

$H_m$  is the soil thickness (cm),  $\theta_m$  is the gravel fraction size larger than 2 mm (%) of the  $m$  layer,  $A_r$  is the rock exposure around the sample site (%), and  $M_m$  is the moisture in the tested soil samples (%). Meanwhile,  $\theta_m$  and  $A_r$ , equal or greater than 0, and lower than 1.

#### 2.4.2. Analysis Methods

The total concentration of SOC was determined using the potassium dichromate method with  $K_2Cr_2O_7$  oxidation at 170–180 °C followed by titration with  $Fe_3O_4$  [37–40]. Data management and statistical analyses were performed using Microsoft Excel 2003, R 2.9.2, IBM SPSS Statistics 22 for Windows and Origin 8.6. The relationships among rocky desertification, SBD, SOC content and different environmental factors (slope position, gradient, aspect, vegetation and soil lithology) were analyzed using redundancy analysis (RDA) and Pearson correlation analysis. RDA is an important method of constrained ordination, and may be used to analyze environmental factors in response to the structure of species and to reflect the correlations among samples, species and environmental factors. The different impact factors were sorted with the gradient boosting decision tree (GBDT) model according to their effects on the SOC. The GBDT is a machine learning decision tree model for various types of data, and has a high accuracy rate.

### 3. Results

#### 3.1. Soil Properties in Different Karst Landforms

The rocky desertification process was characterized by calculating the percentage of rock outcrops at the surface. SBD is an important index of soil quality and the degree of pedogenesis, and these two important factors influence the spatial distribution characteristics of SOC in karst mountain areas [22,41]. Information on the SBD and rock outcrops in different karst landforms is presented in Figure 1. The SBD gradually increased with increasing soil depth in the topsoil layers (0–40 cm). The SBD in the 0–5 cm soil layer ranged from 1.13  $g \cdot cm^{-3}$  to 1.19  $g \cdot cm^{-3}$  in the different karst landforms. The lowest SBD value was found in KC, and the highest value was found in KPCD. The SBD values in the 30–40 cm soil layer ranged from 1.32  $g \cdot cm^{-3}$  to 1.41  $g \cdot cm^{-3}$ , and the lowest value was observed in the KC. The highest values were found in KLH and KTV. SBD values in the top several soil layers were generally higher in KPCD and KPB than the other karst landforms. However, the SBD in the KC was generally lower than the other karst landforms. The SBD increased slowly in subsoil layers at 40–100 cm, with the exception of KLH, and there were no obvious differences in SBD in the same soil layer among different karst landforms. The coefficients of variation of SBD in different karst landforms ranged between 0.07 and 0.23, which indicates low to moderate variation levels. The discrepancy in SBD in the upper soil layers was generally higher than in the subsoil (Figure 1a). There were some discrepancies in rock outcrops among different karst landforms, and the rock exposure of different karst landforms was primarily lower than 20%, except for KC. The percentage of low-degree rock exposure in different karst landforms was between 16% and 65%, and the landforms in order of decreasing rock exposure were KPB > KTV > KLH > KPCD > KC. The low–medium level of rock exposure was between 15% and 34%, and the landforms in order of decreasing rock exposure were KC > KPCD > KLH > KTV > KPB. Areas with rock outcrop percentages that ranged from 0–40% in the different karst landforms accounted for 50% to 85% of the total area, indicating that a low to medium levels of rock outcrop exposure was the main distribution characteristic. However, rock outcrops were generally more abundant in the KC than the other karst landforms, and the rocky desertification of the KC was high (Figure 1b).

#### 3.2. The Statistics of SOC and SOCD in Different Karst Landforms

Statistical information on SOC and SOCD in different karst landforms is listed in Table 2. The spatial distribution characteristics of SOC in the vertical direction exhibited a regular pattern in which the SOC decreased with soil depth. This pattern showed that the SOC quickly decreased in the upper 0–50 cm soil layers, and the reduction rate in the

50–100 cm subsoil layers was significantly lower than the upper 50–100 cm soil layers. The average SOC content in the 0–5 cm soil layer was 30.02 g·kg<sup>-1</sup>, and only 5.72 g·kg<sup>-1</sup> in the bottom soil layer. The discrepancy reached 5.25 times between the surface and bottom soil layers. The different karst landforms in descending order of the SOC range from the surface to the bottom soil layer were KTV > KLH > KC > KPCD > KPB, and their respective ranges were 32.61, 32.13, 28.89, 19.66 and 19.17 g·kg<sup>-1</sup>. At the 0–30 cm soil depth, the SOC content in the different karst landforms decreased in the following order: KLH > KTV > KC > KPCD > KPB. The descending order in the 40–60 cm soil layer was KC > KTV > KLH > KPCD > KPB. However, there was no distinct regular spatial distribution of SOC among the different karst landforms in the 60–100 cm subsoil layer.

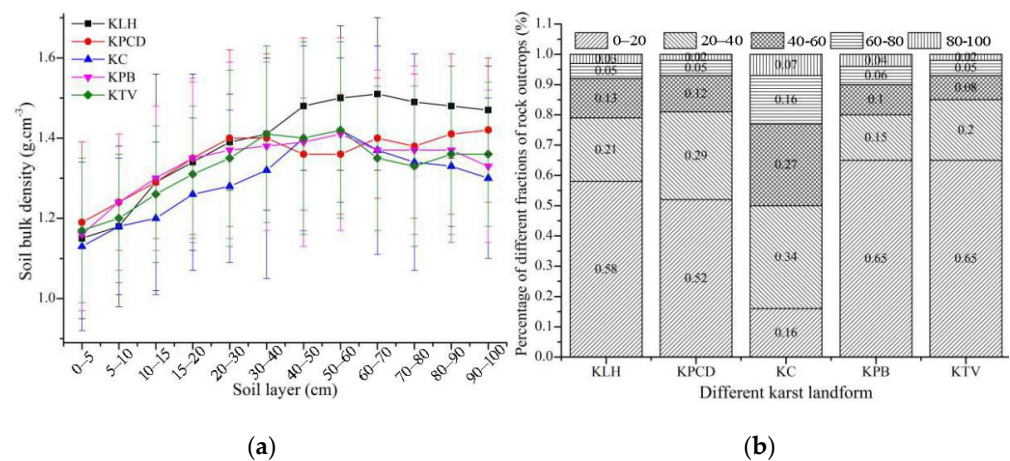


**Figure 1.** Information on SBD and rock outcrops in different soil layers. Panel (a) shows the SBD in different soil layers; panel (b) shows the percentages of rock outcrop exposure in different karst landforms.

**Table 2.** The spatial distributions of SOC and SOCD in soil profiles on different karst landforms.

Depth (cm)	KLH	KPCD	KC	KPB	KTV	Mean	
							SOC (g·kg <sup>-1</sup> )
0–5	38.20 ± 3.12eE	27.08 ± 3.13fB	35.17 ± 3.57gD	23.79 ± 2.39fA	37.85 ± 3.95hED	30.02 ± 2.95gC	
5–10	32.39 ± 3.35dC	24.03 ± 2.91eBA	28.47 ± 3.29fCB	21.61 ± 2.57eA	32.08 ± 3.37gC	26.86 ± 2.32fB	
10–15	29.77 ± 2.83dC	20.64 ± 2.59 dB	25.19 ± 3.36eC	17.56 ± 2.36dA	28.34 ± 2.62fD	23.12 ± 2.63eCB	
15–20	27.79 ± 2.66dE	17.86 ± 2.12cB	22.91 ± 2.63edDC	14.47 ± 2.53cA	24.87 ± 2.75eD	20.29 ± 2.75dC	
20–30	20.58 ± 2.57cC	14.36 ± 2.05cbBA	19.77 ± 2.15dC	12.31 ± 2.12cbA	20.52 ± 2.38dC	16.32 ± 2.16cB	
30–40	13.98 ± 1.59bB	10.63 ± 2.23bA	14.78 ± 2.07cB	10.07 ± 2.08bA	14.16 ± 2.14cB	11.79 ± 1.97bA	
40–50	10.97 ± 1.67baCB	9.78 ± 1.69baB	11.48 ± 2.12cbC	7.76 ± 1.39baA	11.47 ± 1.56bC	9.39 ± 1.65baB	
50–60	9.62 ± 1.82baC	8.31 ± 1.57baB	10.74 ± 1.99bC	6.16 ± 1.67aA	8.66 ± 1.69baB	7.99 ± 1.44baB	
60–70	7.69 ± 1.53aB	7.68 ± 1.39baB	9.63 ± 2.31baC	5.79 ± 1.69aA	6.92 ± 1.33aB	7.05 ± 1.41baB	
70–80	7.56 ± 1.39aC	7.22 ± 1.67aC	9.35 ± 2.12baD	5.45 ± 1.35aA	5.29 ± 1.25aA	6.50 ± 1.37aB	
80–90	7.05 ± 1.30aC	7.08 ± 1.66aC	7.82 ± 1.98aD	5.10 ± 1.52aA	5.07 ± 1.30aA	6.17 ± 1.52aB	
90–100	6.16 ± 1.35aB	6.43 ± 1.35aB	6.28 ± 1.34aB	4.62 ± 1.28aA	4.64 ± 1.07aA	5.72 ± 1.29aBA	
			SOCD (kg·m <sup>-2</sup> )				
0–10	2.51 ± 0.63aA	2.39 ± 0.61aA	2.04 ± 0.68aA	2.18 ± 0.51aA	2.79 ± 0.62aA	2.35 ± 0.65aA	
0–20	4.56 ± 0.93bB	4.35 ± 0.69bBA	3.62 ± 0.94baA	3.85 ± 0.75bA	4.86 ± 0.78bB	4.19 ± 0.82bBA	
0–30	5.70 ± 1.12cbBA	5.72 ± 1.23cbBA	4.86 ± 1.13bA	5.11 ± 0.98cA	6.2 ± 1.39cbB	5.45 ± 1.15cbBA	
0–40	6.30 ± 1.05cBA	6.76 ± 1.12cB	5.66 ± 1.01cbA	6.13 ± 1.30dcBA	6.73 ± 1.67cB	6.28 ± 1.21cBA	
0–50	6.73 ± 1.37dcBA	7.60 ± 1.37dc B	6.11 ± 1.25cA	6.79 ± 1.65dBA	7.12 ± 1.25dcBA	6.85 ± 1.39cBA	
0–60	6.97 ± 1.69dcBA	8.31 ± 1.39dC	6.48 ± 1.68cA	7.23 ± 2.32dB	7.32 ± 2.12dcB	7.24 ± 1.95dcB	
0–70	7.14 ± 2.12dBA	8.97 ± 1.25dC	6.67 ± 2.01cA	7.61 ± 2.07edB	7.47 ± 2.01dB	7.56 ± 2.08dcB	
0–80	7.22 ± 1.98dBA	9.58 ± 2.33edC	6.83 ± 2.32cA	7.95 ± 1.95eB	7.60 ± 2.33dB	7.83 ± 2.12dB	
0–90	7.31 ± 2.03dA	10.21 ± 2.59eC	6.94 ± 2.17dcA	8.25 ± 2.32eB	7.73 ± 1.95dA	8.09 ± 2.31dB	
0–100	7.37 ± 2.37dA	10.79 ± 2.91eC	7.06 ± 2.63dA	8.51 ± 2.56eB	7.84 ± 2.30dBA	8.31 ± 2.44dB	

Notes: Within columns, values followed by the same lowercase letter (a–g) are not significantly different ( $p < 0.05$ ); within rows, values followed by the same capital letter (A–E) are not significantly different ( $p < 0.05$ ).

The SOCD accumulation value increased with soil thickness, while the average growth rate decreased with soil depth. The increased range of SOCD was significant in each soil layer from the surface to a 40-cm soil depth, and was small in subsoil layers of 50–100 cm for all studied karst landforms. The SOCD range in the 0–10 cm soil layer in the different

karst landforms was only  $0.72 \text{ kg}\cdot\text{cm}^{-2}$ . However, this range reached  $3.73 \text{ kg}\cdot\text{cm}^{-2}$  in the 90–100 cm soil layer. From the 0–10 cm soil depth to the 0–100 cm soil depth, the greatest increase in SOCD was observed in KPCD, and the smallest increase was found in KLH. The descending order of the other karst landforms was  $\text{KPB} > \text{KTV} > \text{KC}$ .

### 3.3. The Spatial Distribution Characteristics of Rocky Desertification

The rocky desertification degree was characterized by calculating the rock outcrop percentage. Higher rock outcrop percentages indicate a higher rocky desertification degree. The relationships between rocky desertification and different impact factors including slope position, gradient, aspect, vegetation, and lithology were analyzed. The average rock outcrop percentages in zones I, II, III and IV were 8%, 24%, 29% and 15%, respectively, which indicates that the rocky desertification degree first increased, then decreased slightly. The degree of rocky desertification in zones I and II was lower than in zones III and IV. Zone I primarily included flat ground and depressions in which the soil was generally thick. Zone II was located primarily in the mountain foothills, and these regions were generally covered with lush vegetation, especially trees and shrubs. The rocky desertification of zone III was the worst among all of the zones. Vegetation was sparse and less diverse in this zone of mountains. The slope gradient, which is closely associated with soil erosion, was greater in this region than in the other zones. Notably, the rocky desertification of zone IV was slightly lower than zone III. The following reasons may contribute to this phenomenon: (a) the effects of human disturbance in the upper part of the mountains were weaker; (b) the mountain tops in this area were flatter than in zone III; and (c) this area of the mountains is generally covered with vigorous vegetation, primarily shrubs and grass (Figure 2a).

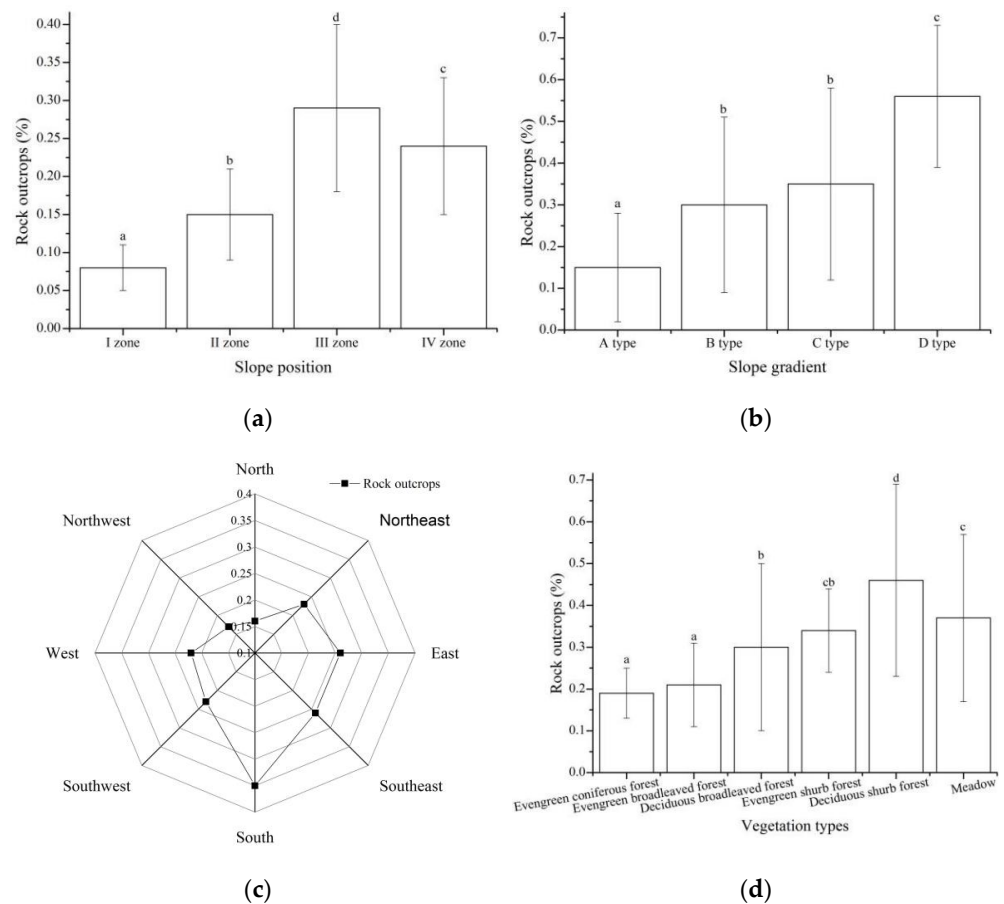
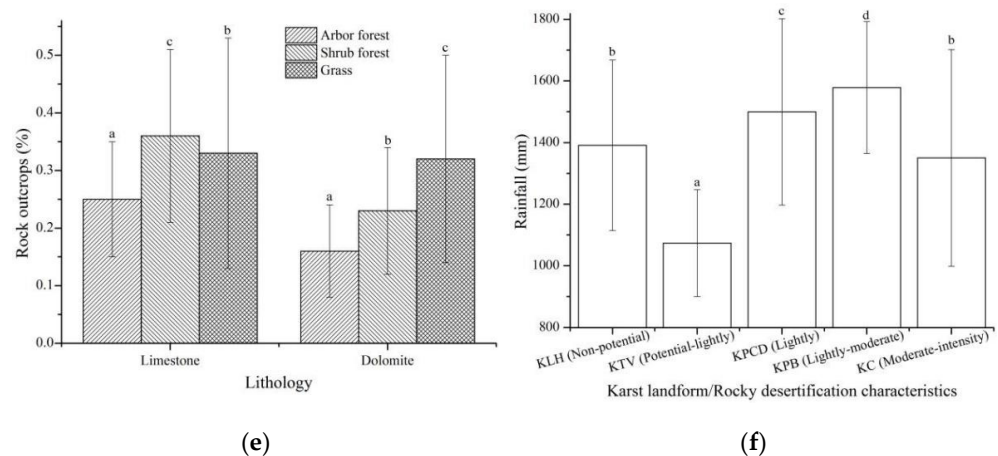


Figure 2. Cont.



**Figure 2.** Information on rocky desertification: (a–e) show the rock outcrops at different slope positions, slope gradients, slope aspects, vegetation and lithologies, respectively; (f) shows the relationship between rainfall and rocky desertification.

There was a distinct discrepancy in rocky desertification at different slope gradient levels (Figure 2b). The rock outcrops increased with increasing slope gradient, indicating a gradually increase of rocky desertification with slope gradient. The rocky desertification related to different slope gradients was divided into three gradient levels. The A type rock outcrops were the first level, B and C types belonged to the second level, and D type was the third level. For low rocky desertification degrees, the spatial discrepancy was relatively low. Significant discrepancies were found among rock outcrops with different slope aspects, and the average rock outcrop ratios of different slope aspects ranged from 0.18 to 0.35. The different slope aspects in order of decreasing rock outcrop area were south (0.35) > southeast (0.31) > east (0.26) = southwest (0.26) > northeast (0.23) = west (0.23) > northwest (0.21) > north (0.18) (Figure 2c). Rock outcrops gradually increased with the retrogressive succession of vegetation; the different vegetation types in decreasing order of rock outcrop area were deciduous shrub forest > meadow > evergreen shrub forest > deciduous broadleaved forest > evergreen broadleaved forest > evergreen coniferous forest. The rock outcrops under evergreen coniferous forest and evergreen broadleaved forest were similar, and their rocky desertification degrees were low. The rocky desertification degrees of shrub forest and meadow were greater than the other vegetation types (Figure 2d). In summary, the variation in rock outcrops under deciduous forest was greater than under evergreen forest, the main reason being that the coverage of a deciduous forest changes seasonally.

The lithological properties of the underlying geological layers (strata) are the basis of soil formation, and are an important factor in rocky desertification occurrence. The main components of carbonate in karst areas include limestone and dolomite. Carbonate rock is easily eroded, especially under acidic conditions, which worsens soil erosion. The rock outcrop percentages in areas underlain by limestone were higher than areas underlain by dolomite under the same vegetation type. For limestone bedrock, the vegetation types in order of by rocky desertification degree were shrub forest > grass > tree forest, and the order for dolomite bedrock was grass > shrub forest > tree forest (Figure 2e). Climate change, especially changes in rainfall, can influence the processes involved in rocky desertification. In order of decreasing average annual rainfall, the landforms in the study regions were KPB > KPCD > KLH > KC > KTV, and in order of rocky desertification degree the landforms were KC > KPB > KPCD > KTV > KLH (Figure 2f). The distribution characteristics of rainfall and rocky desertification were consistent to a certain extent. Vegetation affected the rocky desertification of different karst landforms. Therefore, there were some differences between the landform order for rainfall and rocky desertification. For example, while the rainfall in KLH was higher than KTV and KC, the rocky desertification in KLH was the lowest because of the abundant vegetation.

### 3.4. Factors Affecting the Distribution Characteristics of SBD

According to the SBD information in Figure 1a, the SBD gradually increased from the surface soil layer to a depth of 40 cm, while the trend in the 40–100 cm soil layer in different karst landforms differed. Different factors affected the SBD in the 0–40 cm soil layers. The SBD increased gradually with soil depth at each slope position, and there was a significant regular spatial distribution of SBD at different slope positions with a decreasing order of zone II > zone I > zone III > zone IV. This phenomenon suggests that the SBD values in flat ground and the lower part of the mountain are higher than the upper parts of the mountain (Figure 3a). However, there was no significant regular distribution of SBD in each soil layer under the influence of the slope gradient. The SBD values of the A type, B type and C type were distinctly higher than the D type in the 0–5 cm soil layer. The SBD in the A type was significantly higher than the other slope gradient types in the 5–10 cm soil layer, and these values in the B type, C type and D type were similar. The spatial distribution of SBD in each soil layer from 10–30 cm was the same under different slope gradients, and the descending order of SBD in different slope gradients was A type > C type > B type > D type. The distribution trend of SBD in the 30–40 cm soil layer was A type > B type > C type > D type (Figure 3b). In summary, there were few differences in SBD in the surface soil layers, and the SBD gently decreased with increasing slope gradient in the lower soil layer. The difference in SBD in different slope aspects was small except in the east and southeast aspects. The SBD values in the east and southeast aspects were significantly higher and lower than the other slope aspects, respectively. Overall, the descending order of SBD in different slope aspects was east > west > southwest > south > northwest > north > northeast > southeast, and the average SBD on sunny slopes was generally slightly higher than shady slopes (Figure 3c). There was a regular spatial distribution characteristic of SBD under the influence of different vegetation types. The SBD values under evergreen coniferous forest, evergreen broadleaved forest and deciduous broadleaved forest were similar, and their SBD values were assigned to the first level. The SBD values under evergreen shrub forest, deciduous shrub forest and grass belonged to the second level, and the SBD values of the first level were significantly lower than the second level, indicating that the SBD under tree forest was generally lower than under shrub and grass. There was a regular distribution of SBD in different vegetation types in the second level, i.e., evergreen shrub forest > deciduous shrub forest > grass. The SBD values under evergreen forests were slightly higher than under deciduous forests (Figure 3d). In order to analyze the impact of lithology on the SBD, the SBD distribution characteristics driven by the two main rock types, i.e., limestone and dolomite, under different vegetation types were investigated. The SBD over dolomite bedrock was higher than the SBD over limestone bedrock, and there was a significant regular distribution of SBD under different vegetation types on the same bedrock, i.e., grass > shrub forest > tree forest (Figure 3e). There was a negative correlation between SBD and rock outcrops ( $n = 356$ ,  $r = -0.18$ ,  $p < 0.01$ ), which indicates that a higher rocky desertification degree limits the increase in SBD (Figure 3f).

### 3.5. The SOC Content Response to Different Factors

Different factors influenced the SOC contents, and their spatial distribution characteristics coupled with the process of rocky desertification are listed in Figure 4. The SOC content decreased quickly and regularly in each soil layer from the surface to a depth of 50 cm at different slope positions. The descending order of SOC content at different slope positions in the 0–40 cm soil layer was zone II > zone I > zone III > zone IV > zone III, which reveals that the SOC gradually increased at first, then quickly decreased, and finally increased slightly from flat ground to mountain foot to mountain top, respectively. The SOC contents in zones I and II were generally higher than zones III and IV in the 40–100 cm soil layer, and the discrepancies in the SOC contents in the subsoil layers were lower than the upper soil layers (Figure 4a). This discrepancy occurred because the soil thickness in flat ground and the mountain foot was thick, and the vegetation was more abundant. However, humans disturbed mountaintops less, and the SOC accumulated under the influence of

the microtopography. The distribution characteristics of the SOC contents in response to different slope gradients are shown in Figure 4b. The descending order of SOC content in each soil layer in the 0–30 cm layer among the different slope gradients was B type > C type > D type > A type. The SOC content quickly increased from the A type to the B type, and the SOC content in the B type was significantly higher than the other slope gradient groups. There was a lack of a significant regular distribution in SOC content in the subsoil layer at different slope gradients, except that the SOC content in the D type was generally slightly higher than the other slope gradient groups. The distribution characteristics of the SOC content in different slope gradients showed that the SOC content along the slope gradient first increased, then decreased. This distribution phenomenon of SOC content was a result of the contribution of some advantageous microtopographies such as rock basins, grooves, and crevices. Microtopography provides an advantageous place for the accumulation of organic matter, including the branches and leaves of trees and the bodies and feces of animals. To analyze the SOC content response to changes in slope aspect, the relationship between SOC content and different slope aspects was analyzed. The results showed that the descending order of SOC content in different slope aspects was north > northwest > east > northeast > west > southwest > south > southeast (Figure 4c). In summary, the SOC content in the northern aspect of the mountain was higher than the other slope aspects, while the SOC content in the south aspect was generally lower than the other slope aspects. This phenomenon occurred because the geographic environments of the different slope aspects were different. There were some differences in SOC content in different soil layers under different vegetation types. The descending order of SOC content in different vegetation types in the 0–30 cm soil layer was deciduous broadleaved forest > evergreen broadleaved forest > evergreen coniferous forest > deciduous shrub forest > evergreen shrub forest > grass. The descending order of SOC content in the 30–100 cm soil layer was evergreen coniferous forest > evergreen broadleaved forest > deciduous broadleaved forest > evergreen shrub forest > deciduous shrub forest > grass (Figure 4d). Evergreen coniferous, evergreen broadleaved and deciduous broadleaved trees all form tree forests, and the SOC content in soils under tree forest was generally greater than shrub forest areas and grassland. The average SOC content in soil originating from limestone bedrock was greater than soil originating from dolomite. The SOC content in soil originating from limestone was greater than soil originating from dolomite under all different vegetation types (Figure 4e). The rock outcrops and SOC contents of soils originating from limestone were greater than soils originating from dolomite. This result is due to limestone being easily eroded, and because its microtopography (stony basin, stony trough, stony gully, etc.) is more complex than that of dolomite; favorable terrain promotes enrichment of SOC. There was a significant negative correlation between SBD and SOC content ( $n = 838$ ,  $r = -0.28$ ,  $p < 0.01$ ). However, the relationship between rock outcrops and SOC content was slightly positive ( $n = 358$ ,  $r = 0.15$ ,  $p < 0.05$ ) (Figure 4f,g). This result likely indicates that a certain lower level of rock outcrops promotes SOC accumulation, which comes from the contribution of gathering effects. Therefore, the SOC concentration increased from lower to moderate degrees of rocky desertification. When rocky desertification became intense, the SOC concentration rapidly decreased (Figure 4h). The relationships between SOC content and different impact factors are presented in Figure 5i. The factors affecting the SOC in the 0–5 cm and 5–10 cm soil layers were similar. The main factors affecting the SOC in the 10–15 cm and 15–20 cm soil layers were similar, and the SOC content of the soil at the soil–bedrock interface was highly impacted by lithology. Based on gradient boosting decision tree (GBDT) analysis, the descending order of different factors was rock outcrops > SBD > vegetation > lithology > slope position > slope gradient > slope aspect, and their percentage contributions were 33.76%, 30.34%, 17.96%, 8.64%, 4.55%, 2.80% and 1.95%, respectively (Figure 4j). In summary, the slope position, gradient and aspect affected SOC by influencing plant growth, SBD and rocky desertification. Therefore, slope position, gradient and aspect are indirect influencing factors, and vegetation, rocky desertification and SBD are direct influencing factors of the SOC content.

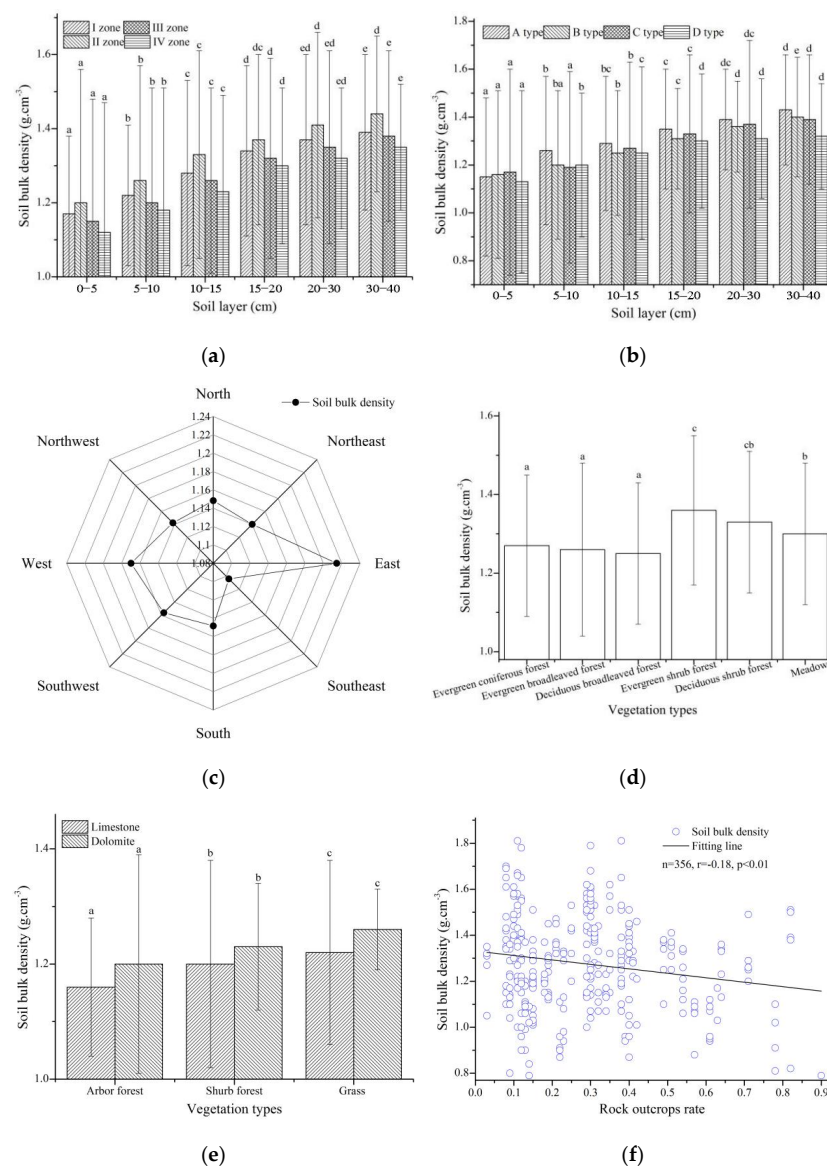


**Figure 3.** Information on SBD: (a–f) show the relationship between SBD and slope position, gradient, aspect, vegetation, lithology and rock outcrops, respectively.

### 3.6. The SOCD Spatial Distribution Characteristics

The spatial distribution characteristics of the SOCD response to different slope positions showed an obvious regular distribution of SOCD in most soil profiles. The descending order of SOCD at different slope positions in all soil profiles was zone II > zone I > zone III > zone IV. There was a significant increase in SOCD in the 0–50 cm layers, with increasing soil thickness at all slope positions. Especially at 10–20 cm, the SOCD increased considerably. The increase in SOCD was small in the 50–100 cm soil layer at different slope positions (Figure 5a). The discrepancies in SOCD among the slope positions gradually increased with increasing soil thickness. There was a greater discrepancy in SOCD at different soil depths, which was driven by the slope gradient. The difference in SOCD with different slope gradients was slight in the topsoil layer (0–10 cm), and the SOCD range among different slope gradients was only  $0.18 \text{ kg} \cdot \text{m}^{-2}$ . The descending order of SOCD in the 0–30 cm soil layer for different slopes was C type > A type > B type > D type, and the SOCD range was  $0.63 \text{ kg} \cdot \text{m}^{-2}$ . From the 0–30 to 0–100 cm soil layers, the descending order of SOCD for different slopes was A type > C type > D type > B type, and the SOCD range reached  $3.51 \text{ kg} \cdot \text{m}^{-2}$  (Figure 5b). Therefore, there was no stable order of SOCD among

different slopes with increasing soil thickness. The range of SOCD increased gradually with increasing soil depth. In summary, the discrepancy in SOCD among different slopes increased gradually with increasing soil thickness, and the SOCD for gentle slopes was generally greater than steep slopes. The distribution information of SOCD in the 0–20, 0–50, and 0–100 cm soil layers with different slope aspects is shown in Figure 5c. The descending order of SOCD in the 0–20 cm soil layer in different slope aspects was north > northwest > northeast > west > east > southwest > southeast > south, and the SOCD range was 0.52 kg·m<sup>-2</sup>. The descending order of SOCD in the 0–50 cm soil layer in different slope aspects was north > west > northeast > east > northeast > southwest > southeast > south; this order was slightly different from the 0–20 cm layer. The SOCD range was 0.77 kg·m<sup>-2</sup>. The SOCD in the 0–100 cm soil layer for different aspects ranged from 6.72 to 9.39 kg·m<sup>-2</sup>, and the descending order for different slope aspects was similar to the 0–20 cm soil layer. In summary, the SOCD in the north aspect was greater than in the other slope aspects, while, the SOCD in the south aspect was generally lower than in the other slope aspects. Because the north aspect was a shady slope, its vegetation and soil thickness were greater than the south aspect. The south aspect was a sunny slope, and its rocky desertification was generally more severe than the other slope aspects. There was a significant regular distribution of SOCD with change in the rocky desertification process. The SOCD decreased gradually with aggravation of the rocky desertification degree. The discrepancy in SOCD at different rocky desertification levels gradually increased with soil depth. There was little difference in SOCD in the 0–20 cm soil layer at different degrees of rocky desertification, and the range was only 0.71 kg·m<sup>-2</sup>. The SOCD range of the 0–100 cm soil layer reached 5.93 kg·m<sup>-2</sup>, which was 8.36 times greater than the 0–20 cm soil layer. The accumulation of SOCD from the surface soil layer (0–20 cm) to the subsoil layer (0–100 cm) in light rocky desertification areas was significant, but it was not distinct in severe rocky desertification areas (Figure 5d).

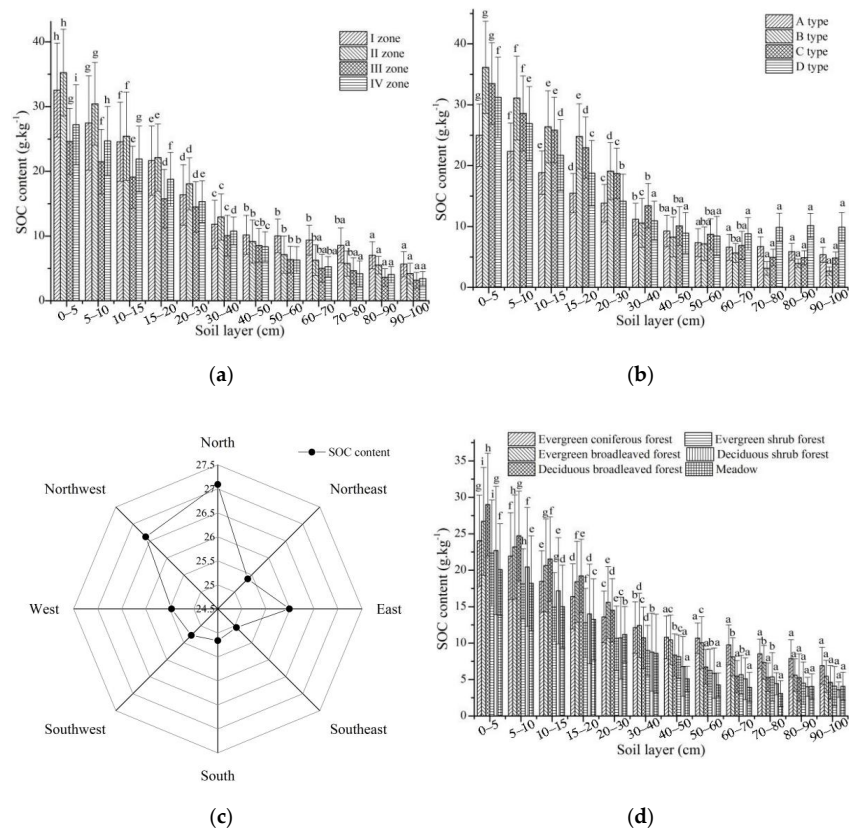
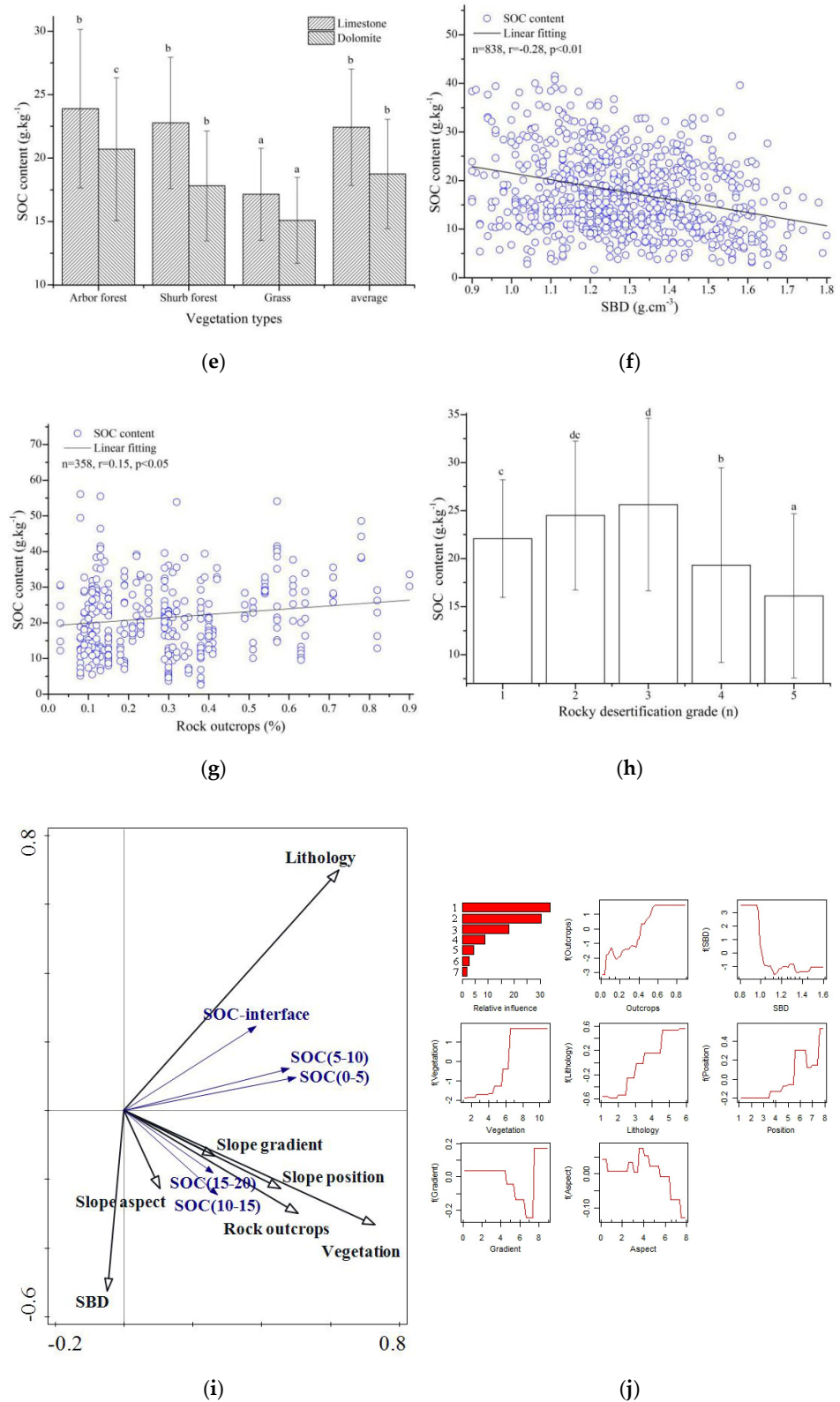
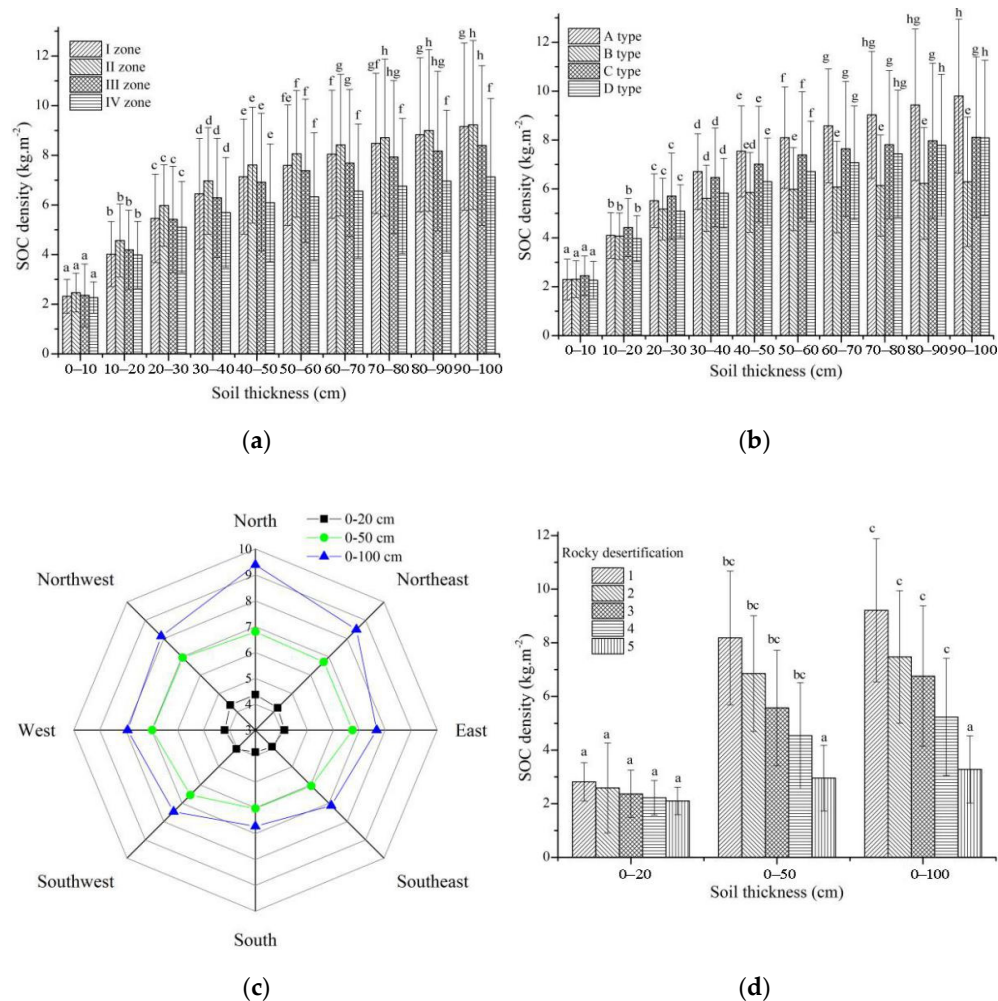


Figure 4. Cont.



**Figure 4.** The spatial distribution characteristics of SOC are affected by different factors: (a–h) show the relationship between SOC content and slope position, gradient, aspect, vegetation, lithology, SBD, rock outcrops and changes in rocky desertification, respectively; (i) shows the RDA of the SOC content in the main soil layer and different impact factors; (j) shows the sorting of different factors affecting the SOC content by GBDT.



**Figure 5.** Information on SOCD spatial distribution characteristics: (a–c) show the SOCD at different slope positions, gradients and aspects; (d) shows the change trend of SOCD in several main soil layers during the rocky desertification process.

### 3.7. The Evolution Characteristics of SOC Storage Capability

The microtopography is complex under karst landforms, and soils are noncontinuous and shallow. The rocky desertification degree of different karst landforms is different, which results in discrepancies of SOC storage capacity. SOC storage is characterized by SOCD; thus, the changes in SOCD trends can help to evaluate the characteristics of SOC storage capacity evolution in soil. The SOCD of each soil layer in the vertical direction first increased, then decreased gradually. SOCD reached its peak value in the 5–10 cm soil layer. This result indicates that the SOC storage capacity in the 5–10 cm soil layer was the greatest. The SOC storage capacity of the deeper soil layers decreased gradually to the 40–50 cm soil layer. Little difference existed in the SOC storage capacity among the different soil layers from 50–100 cm. However, the discrepancy in SOC storage capacity increased gradually from the 0–5 cm to the 90–100 cm soil layer, and all of the variation coefficients exhibited high variation (Figure 6a). To analyze the SOC storage capacity in different karst landforms, SOCD in similar environments and microtopographies was compared within different karst landforms. The SOC storage capacity of different karst landforms in the 0–30 cm soil layer decreased in the order KTV > KLH > KPCD > KC > KPB. The SOC storage capacity in the 0–50 cm soil layers of KLH and KTV was significantly greater than in the other karst landforms. The SOC storage capacity in KPCD and KPB were similar, and the SOC storage capacity in KC was significantly lower than in the other karst landforms. The SOC storage capacity in the 0–100 cm layer of KPCD was slightly greater than KPB, and both

areas belonged to the first gradient level. The SOC storage capacity in KLH was similar to KTV, and both areas belonged to the second gradient level. The SOC storage capacity in the KC was the third gradient level, and its SOC storage capacity was significantly lower than the other karst landforms (Figure 6b). The SOCD decreased with increasing rocky desertification degree, and the SOC storage capacity gradually decreased in the low rocky desertification classes, that is, classes 1–3. From class 3 to class 5, the SOC storage capacity sharply decreased (Figure 6c). For further study of the SOC storage capacity of different karst landforms coupled with rocky desertification, the percentage of the SOCD fraction of different karst landforms with different rocky desertification degrees was determined. The descending order of SOCD proportion for rocky desertification degree of grade 1 in different karst landforms was KLH (71%) > KPCD (68%) > KTV (67%) > KPB (63%) > KC (56%). The descending order of SOCD proportion for rocky desertification degree of grade 2 in different karst landforms was KC (17%) > KPB (16%) > KPCD (15%) > KTV (14%) > KVF (13%). The SOC storage capacity contributions in the different karst landforms were primarily associated with rocky desertification grades 1 and 2, and their contribution rates were 86% (KLH), 83% (KPCD), 73% (KC), 79% (KPB) and 81% (KTV). The SOC storage capacity contribution rate of high rocky desertification (grades 4 and 5) was higher for KC than the other karst landforms (Figure 6d). These results indicate that SOC storage capacity is primarily associated with low rocky desertification areas for all karst landforms.

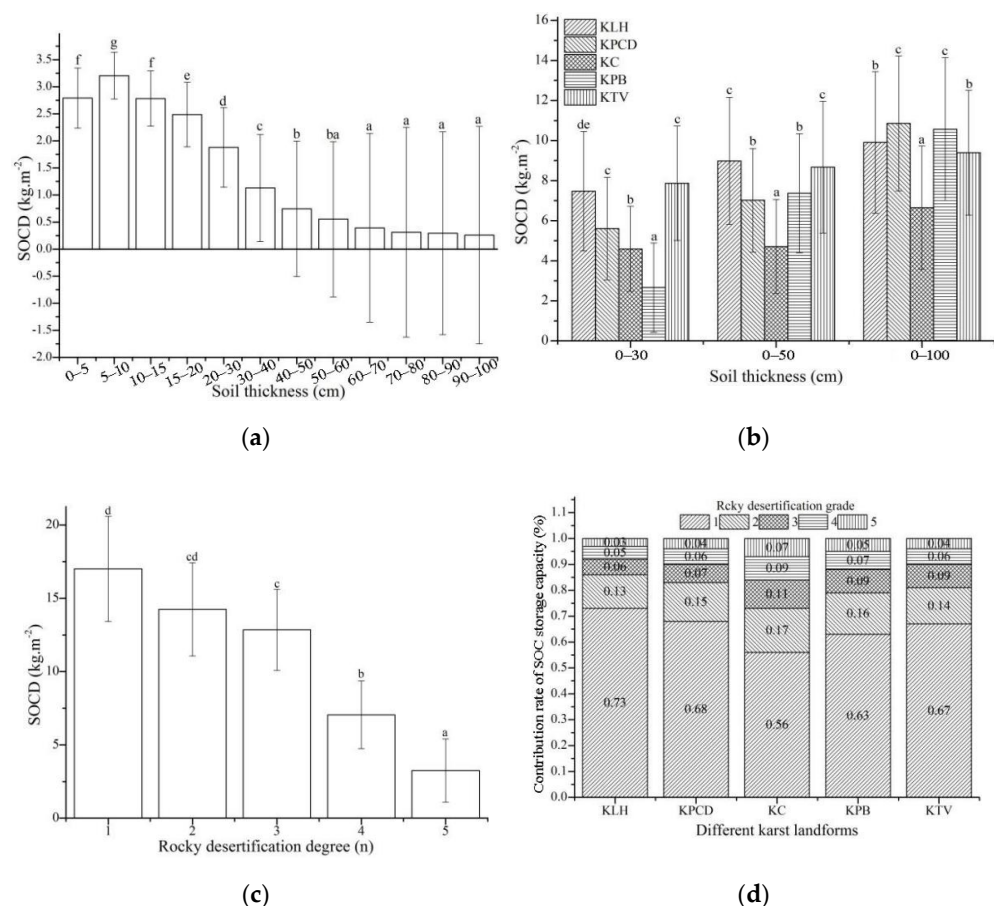


**Figure 6.** Information on SOC storage capacity spatial distribution. Panel (a) shows the vertical distribution of SOCD; (b) shows the SOCD in different karst landforms; (c) shows the change trend of SOCD with rocky desertification process; (d) shows the percentage of SOC storage capacity contribution in different rocky desertification degrees in different karst landforms.

## 4. Discussion

### 4.1. The Relationships among SOC, SBD and Rocky Desertification Processes in Karst Areas

SOC, SBD and rocky desertification are important indexes of soil and the eco-environment in karst areas [16,19]. The relationships among rocky desertification, SBD, SOC and SOCD were analyzed using Pearson correlation analysis (Table 3). SBD is an important index of the degree of soil maturation, and the SBD of raw soil is generally higher than mature soil. Because rocky desertification aggravates soil erosion, weathered soil covers the bedrock. However, the relationship between SBD and rocky desertification may be discussed in two aspects. First, the density of raw soil from weathered bedrock is greater than mature soil. Therefore, the density of soil in rocky desertification areas is theoretically higher than in nonrocky desertification areas. Second, microtopography in rocky desertification areas is favorable for gathering soil and organic matter. Therefore, soil in microtopography has a low SBD and a high SOC content [21]. This distribution may be the reason SBD was negatively correlated with rocky desertification and why SOC content was positively correlated with rocky desertification. Rocky desertification reflects the intensity of human disturbance. Organic matter easily infiltrates the deep soil layer. However, organic matter is easily washed away by heavy rain in areas with severe rocky desertification [15,19]. SOCD was negatively correlated with rocky desertification. The correlation coefficient between SBD and SOC was  $-0.367^{**}$ , which indicates that SBD is an important factor in limiting the SOC content in soils [16]. In contrast, a significant positive correlation was found between SBD and SOCD, a result which is consistent with Huang [22] and Wang [27].

**Table 3.** Pearson correlation analysis of SOC, SOCD, SBD and rock outcrops.

	Rock Outcrops	SBD	SOC	SOCD
Rock outcrops	1			
SBD	$-0.231^{**}$	1		
SOC	0.052	$-0.367^{**}$	1	
SOCD	$-0.172$	$0.076^{**}$	$0.520^{**}$	1

\*\* Correlation is significant at the 0.01 level.

### 4.2. The Transformation of SOC Storage Capacity during the Development of Karst Landforms

The development of karst is based on a long period of geological and climatic stability; the main bedrock composition is carbonate rocks [42]. The bedrock of karst areas is dissolved, which results in landform changes. There are considerable differences in ecology and environment among the different karst landform stages, and the soil erosion strength and rocky desertification characteristics are also different. Therefore, there are great differences in the spatial distribution characteristics and storage capacity of SOC among different karst landforms [15,22]. The rocky desertification distribution characteristics of karst landforms evolves with the succession process of vegetation. In KPB and KTV (stage I), vegetation was destroyed to develop agriculture, resulting in a gradual increase in rocky desertification. Rocky desertification in KC (stage II) reached an even higher level; vegetation was sparse, and soil erosion was severe. The vegetation in KPCD (stage III) gradually recovered, especially shrub forests. The vegetation types in KHL (stage IV) included multiple plant mixtures, including trees, shrubs and grass, and the soil thickness increased. Stage IV areas are good for developing agricultural land and easily disturbed by production activities, which leads to a slight increase in soil erosion. The SOC storage capacity in the different evolution stages of karst landform evolution first decreased, then gradually increased (Figure 7a). The SOC storage capacity in stage II quickly decreased from stage I, then increased sharply in stage III. The rate of increase slowed in stage IV. The SOC storage capacity in different karst landform stages was negatively associated with the degree of rocky desertification. The contribution rate of SOC storage at different soil depths was different in different karst stages. The descending order of the SOC storage contribution rate of the different karst stages in the 0–20 cm soil layer was stage II (0.61) > stage II (0.53) > stage I (0.44) > stage IV (0.41). The descending order in the 20–40 cm soil

layer was stage III (0.28) > stage I (0.27) > stage II (0.24) > stage IV (0.23). However, the descending order in the 40–100 cm soil layer was stage IV (0.36) > stage I (0.29) > stage III (0.20) > stage II (0.14) (Figure 7b). These results reveal that the contribution to SOC storage primarily comes from soils thicker than 40 cm, especially in stage II, and the contribution rate reaches 0.85. For stage II, the upper soil erosion was severe, which led to a decrease in the SOC storage capacity. The soil thicknesses of stages I and IV were thicker than stages II and III. Therefore, the discrepancies in SOC storage capacity in each soil layer in stages I and IV were lower than stages II and IV. Therefore, the stabilities of SOC storage capacity in different soil layers in stages I and IV were greater than stages II and III. The variation in SOC storage capacity related to karst landform evolution stages indicates that SOC storage capacity is closely associated with karst landform evolution.

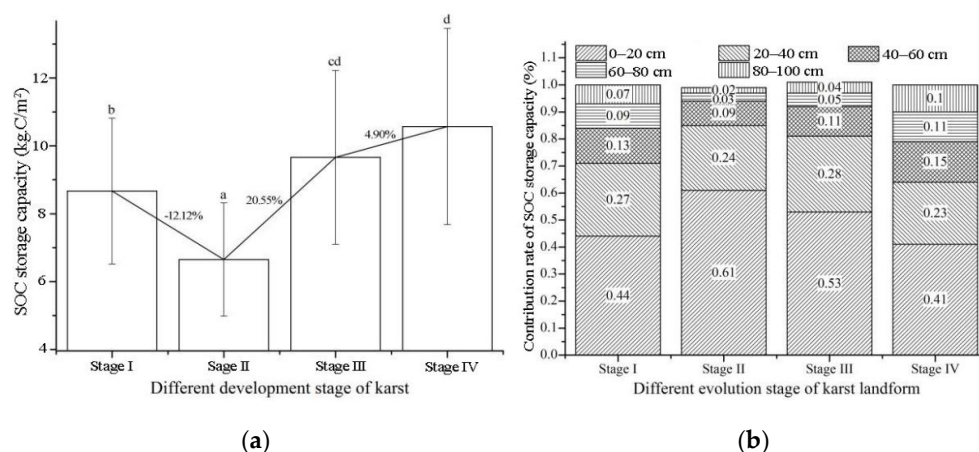


**Figure 7.** Information on SOC storage capacity. Panel (a) shows the change in SOC storage capacity in different karst stages; (b) shows the contribution rate of SOC storage capacity in different soil layers of different karst stages.

#### 4.3. The Reliability of Geographic Environmental Factors in SOC Spatial Reconstruction

According to the information on rocky desertification and the SBD and SOC data shown in Figures 2–4, rocky desertification, SBD and vegetation directly impact SOC. Vegetation was the key factor for rocky desertification and SBD, and the spatial distribution discrepancies of vegetation were accompanied by changes in slope position, gradient and aspect. In general, the lower rocky desertification of flat ground and mountain foothill areas resulted in greater soil thickness and lush vegetation. In contrast, the middle and upper parts of the mountains featured a simple and unitary environmental structure that led to higher degrees of rocky desertification. Lower slope gradients were primarily found in flat ground and mountain foothill areas, and the soil in these regions was thicker, more uniform and more continuous. The soil thickness decreased, rock outcrops increased, and vegetation coverage decreased with an increase in slope gradient and the tendency to form steep slopes. The ecological structure became simple and weak thereafter. The southern aspect of mountains in the Northern Hemisphere features sunny slopes, and the northern aspect is associated with shady slopes. On sunny slopes, soil moisture is easily reduced by evaporation, which results in drier, denser and harder soil. The soil fertility on sunny slopes is generally poorer than other slopes. On shady slopes, the sunshine is warm and less intense, and the temperature and evaporation are lower than on sunny slopes, which results in the soil being moist and rich in organic matter. Overall, the vegetation on shady slopes is more lush than sunny slopes. Therefore, the rocky desertification of sunny slopes is generally more serious than shady slopes.

Areas of flat ground are generally cultivated, and chemical fertilizer is widely applied to the soil. Chemical fertilizers include calcium and nitrogen, which improve the SOC storage capacity [43]. These factors may be why the SOC contents in KTV and KLH were greater than the other karst landforms. The soil was thick in mountain foothill areas and

vegetation was abundant, which enhanced organic matter accumulation and soil fertility. The following factors may explain SOC accumulation at mountain summits: (a) the summit is less disturbed, and shrub and grass cover is higher than at the middle elevations of the mountains; (b) the low temperature of the summit leads to a low decomposition rate of SOC; and (c) the microtopography may produce a gathering effect. The impact of rocky desertification and slope gradient on the distribution characteristics of SOC were similar to the changes in SOC with slope position. Areas with gentle slopes are generally used as farmland. Areas with steep slopes are less disturbed and not suitable for agricultural production. A certain slope gradient promotes SOC accumulation under the influence of microtopography (such as rock basins, grooves, crevices, etc.). However, the SOC decreases gradually when the slope gradient exceeds a certain value because rocky desertification becomes more serious. Many other factors including sunshine, temperature, rainfall, wind, soil properties and vegetation vary among different slope aspects. On sunny slopes, the total sunshine is high, the reflectivity is low, and the temperature and evaporation are high, which results in harder, thinner and drier soil. On shady slopes, the temperature and water evaporation are lower, and the soil moisture is generally higher. Vegetation is generally lush on shady slopes compared to sunny slopes, and the soil fertility of shady slopes is higher than sunny slopes. Sunny slopes are directly exposed to the sun, and the decomposition rate of SOC is faster on sunny slopes than shady slopes. Therefore, the SOC content in areas on the north aspect of the mountain is higher than areas on the other slope aspects.

The SOC content in the upper soil horizon of 0–50 cm exhibited some discrepancies related to different slope positions, slope gradients and slope aspects, and its variation coefficients reached a highly variable level. This result is similar to Zhang [14] and Wang [15]. The SOC decreased in the upper 50 cm of soils, and the rate of decrease was low in deeper soils (50–100 cm), which indicates that 50 cm is a key depth for the SOC content in soil profiles. Under the same conditions, the SOC content of forest soil was greater than soils with other land uses. Therefore, forests promote SOC accumulation, especially in the surface soil [36,44]. As shown in Figure 6, the ranges of SOCD at different slope positions, slope gradients and slope aspects were 3.99–4.57 kg·m<sup>-2</sup>, 3.97–4.42 kg·m<sup>-2</sup> and 3.85–4.37 kg·m<sup>-2</sup>, respectively. These values are similar to the results of Huang et al. (2018b). For the 0–100 soil horizon, the SOCD ranges for different slope positions, slope gradients and slope aspects were 7.12 to 9.16 kg·m<sup>-2</sup>, 6.29 to 9.80 kg·m<sup>-2</sup> and 6.71 to 9.39 kg·m<sup>-2</sup>, respectively. All of these values are lower than 10.53 kg·m<sup>-2</sup>, which is the mean SOCD in China [45]. While these values are lower than those for loess hills (10.92 kg·m<sup>-2</sup>) [46], the SOCD spatial distribution characteristics and the associated ranges in the present study are similar to previous studies [26]. The vertical spatial distribution characteristics of SOCD related to different slope positions, slope gradients and slope aspects are similar to the results of Subramanian et al. [47]. All of these results suggest similar spatial distribution characteristics and ranges of SOCD in different karst areas; these characteristics and ranges are different from non-karst landforms.

In summary, based on the present study the distribution characteristics of SOC were directly associated with rocky desertification, SBD, and vegetation, and indirectly associated with slope position, slope gradient, slope aspect, soil lithology and rainfall. Rocky desertification in the evolution process of karst landforms is an important indicator of SOC storage capacity.

## 5. Conclusions

There were some discrepancies in SOC and SOCD among the different karst landforms; the value in the 0–100 cm soil horizon ranged from 4.62 to 38.29 g·kg<sup>-1</sup> and 2.04–10.79 kg·m<sup>-2</sup>. The SOC content decreased quickly in the 0–50 cm soil horizon, and gently in the 50–100 cm soil horizon. From mountain foothills to summit, the SOC content first increased, then decreased quickly, and finally increased slightly. The SOC content generally decreased with increasing slope gradient. However, this regular distribution may

be out of order, sometimes due to microtopography. The SOC content in the northern aspect of mountains was generally higher than the southern aspect. Rocky desertification, soil bulk density and vegetation had direct impacts on the spatial distribution of SOC. Slope position, slope gradient, slope aspect, soil lithology and rainfall were indirect impacting factors. The descending order of different impact factors was rocky desertification > soil bulk density > vegetation > soil lithology > slope position > slope gradient > slope aspect. The increased range of SOCD was significant in each soil layer from the surface to a 40 cm soil depth, and was small in subsoil layers of 50–100 cm for different karst landforms. Rocky desertification was the key indicator of SOC storage in the different evolution stages of karst landforms. During the process of karst landform evolution, the SOC storage capacity decreased during infancy and youth, then increased gradually from youth to maturity. The SOC storage capacity in the youth period was obviously lower than in the infancy and older period. SOC storage capacity was primarily associated with the upper soil horizon (0–40 cm) for all karst landforms, especially karst canyons. The structural stability of SOC storage capacity in the infancy and maturity periods was greater than in youth and middle age, and the anti-interference ability of SOC storage capacity was greater. The relationship between carbon balance and rocky desertification was not considered in this study. Therefore, further studies are needed in order to reveal the transformation of SOC fractions with rocky desertification in order to further support ecosystem services in karst areas.

**Author Contributions:** K.X. and J.H. conceived the research idea and designed sampling plan. X.W. and X.H. conducted field data collection and laboratory analysis and data treatment. Z.Z. and J.Z. All authors have read and agreed to the published version of the manuscript.

**Funding:** This research was supported by the Key Project of Science and Technology Program of Guizhou Province (No. 5411 2017 Qiankehe Pingtai Rencai), the China Overseas Expertise Introduction Program for Discipline Innovation (D17016), the Growth Project of Young Scientific and Technological Talents in Universities of Guizhou Province ([2021] 302), the Science and Technology Department of Guizhou Province (QKH[2019]1217, [2020]1Y178), and the Project funded by China Postdoctoral Science Foundation (2020M673582XB).

**Institutional Review Board Statement:** This study did not involve human or animals.

**Informed Consent Statement:** Informed consent was obtained from all subjects involved in the study.

**Data Availability Statement:** Not available.

**Conflicts of Interest:** The authors declare that they have no known competing financial interests or personal relationships that could have appeared to influence the work reported in this paper.

## References

1. Rodrigo-Comino, J.; Senciales, J.M.; Cerda, A.; Brevik, E.C. The multidisciplinary origin of soil geography: A review. *Earth-Sci. Rev.* **2018**, *177*, 114–123. [[CrossRef](#)]
2. Keesstra, S.D.; Bouma, J.; Wallinga, J.; Tittonell, P.; Smith, P.; Cerdà, A.; Montanarella, L.; Quinton, J.N.; Pachepsky, Y.; Putten, W.H.; et al. The significance of soils and soil science towards realization of the United Nations Sustainable Development Goals. *Soil* **2016**, *2*, 111–128. [[CrossRef](#)]
3. Wu, J.; Stephen, Y.; Cai, L.Q.; Zhang, R.Z.; Qi, P.; Luo, Z.Z.; Li, L.L.; Xie, J.H.; Dong, B. Effects of different tillage and straw retention practices on soil aggregates and carbon and nitrogen sequestration in soils of the northwestern china. *J. Arid L.* **2019**, *11*, 567–578. [[CrossRef](#)]
4. Hobley, E.; Willgoose, G.R.; Frisia, S.; Jacobsen, G. Stability and storage of soil organic carbon in a heavy-textured karst soil from south-eastern Australia. *Soil Res.* **2014**, *52*, 476–482. [[CrossRef](#)]
5. Singh, S.K.; Singh, A.K.; Sharma, B.K.; Tarafdar, J.C. Carbon stock and organic carbon dynamics in soils of rajasthan, india. *J. Arid Environ.* **2007**, *68*, 408–421. [[CrossRef](#)]
6. Keesstra, S.; Mol, G.; Leeuw, J.D.; Okx, J.; Molenaar, C.; Cleen, M.D.; Visser, S. Soil-related sustainable development goals: Four concepts to make land degradation neutrality and restoration work. *Land* **2018**, *7*, 133. [[CrossRef](#)]
7. Visser, S.M.; Keesstra, S.; Maas, G.; Cleen, M.D.; Molenaar, C. Soil as a Basis to Create Enabling Conditions for Transitions Towards Sustainable Land Management as a Key to Achieve the SDGs by 2030. *Sustainability* **2019**, *11*, 6792. [[CrossRef](#)]
8. Scharlemann, J.P.; Tanner, E.V.; Hiederer, R.; Kapos, V. Global soil carbon: Understanding and managing the largest terrestrial carbon pool. *Carbon Manag.* **2014**, *5*, 81–91. [[CrossRef](#)]

9. Akpa, S.I.C.; Odeh, I.O.A.; Bishop, T.F.A.; Hartemink, A.E.; Amapu, I.Y. Total soil organic carbon and carbon sequestration potential in Nigeria. *Geoderma* **2016**, *271*, 202–215. [[CrossRef](#)]
10. Weissert, L.F.; Salmond, J.A.; Schwendenmann, L. Variability of soil organic carbon stocks and soil CO<sub>2</sub> efflux across urban land use and soil cover types. *Geoderma* **2016**, *271*, 80–90. [[CrossRef](#)]
11. Pouyat, R.; Groffman, P.; Yesilonis, I.; Hernandez, L. Soil carbon pools and fluxes in urban ecosystems. *Env. Pollut.* **2002**, *116* (Suppl. S1), S107–S118. [[CrossRef](#)]
12. Niu, X.; Gao, P.; Li, Y.X.; Li, X. Impact of different afforestation systems on soil organic carbon distribution characteristics of limestone mountains. *Pol. J. Env. Stud.* **2015**, *24*, 2543–2552.
13. Zhang, Z.M.; Zhou, Y.C.; Wang, S.J.; Huang, X.F. The soil organic carbon stock and its influencing factors in a mountainous karst basin in P. R. China. *Carbonates Evaporites* **2019**, *34*, 1031–1043. [[CrossRef](#)]
14. Zhang, Z.M.; Zhou, Y.C.; Wang, S.J.; Huang, X.F. Change in SOC Content in a Small Karst Basin for the Past 35 years and its Influencing Factors. *Arch. Agron. Soil Sci.* **2018**, *64*, 1474520. [[CrossRef](#)]
15. Wang, X.F.; Huang, X.F.; Hu, J.W.; Zhang, Z.M. The Spatial Distribution Characteristics of Soil Organic Carbon and Its Effects on Topsoil under Different Karst Landforms. *Int. J. Environ. Res. Public Health* **2020**, *17*, 2889. [[CrossRef](#)] [[PubMed](#)]
16. Yan, J.H.; Zhou, C.Y.; Wen, A.B.; Liu, X.Z.; Chu, G.W.; Li, K. Relationship between Soil Organic Carbon and Soil Bulk Density in the Rocky Desertification Process of Karst Ecosystem in Guizhou. *J. Trop. Subtrop. Bot.* **2011**, *19*, 273–278.
17. Tian, Z.; Wu, X.Q.; Dai, E.F.; Zhao, D.S. SOC storage and potential of grasslands from 2000 to 2012 in central and eastern Inner Mongolia, China. *J. Arid Land* **2016**, *8*, 364–374. [[CrossRef](#)]
18. Huang, X.F.; Zhou, Y.C.; Zhang, Z.M. Carbon Sequestration Anticipation Response to land use change in a mountainous karst basin in China. *J. Environ. Manag.* **2018**, *228*, 40–46. [[CrossRef](#)]
19. Huang, X.F.; Zhou, Y.C.; Zhang, Z.M. Distribution characteristics of Soil Organic Carbon under different land uses in a karst rocky desertification area. *J. Soil Water Conserv.* **2017**, *31*, 215–221.
20. Zhang, Z.M.; Zhou, Y.C.; Wang, S.J.; Huang, X.F. Estimation of soil organic carbon storage and its fractions in a small karst watershed. *Acta Geochim.* **2018**, *37*, 113–124. [[CrossRef](#)]
21. Wang, X.F.; Huang, X.F.; Hu, J.W.; Zhang, Z.M. Relationship Among Soil Organic Carbon and Small Environment and Lithology in the Rocky Desertification process in Different Karst Landforms. *J. Soil Water Conserv.* **2020**, *34*, 295–303.
22. Huang, X.F.; Wang, S.J.; Zhou, Y.C. Soil organic carbon change relating to the prevention and control of rocky desertification in Guizhou Province, SW China. *Int. J. Glob. Warm.* **2018**, *15*, 315–332. [[CrossRef](#)]
23. Hou, G.L.; Delang, C.; Lu, X.X. Afforestation changes soil organic carbon stocks on sloping land: The role of previous land cover and tree type. *Ecol. Eng.* **2020**, *152*, 105860. [[CrossRef](#)]
24. Zhang, X.F.; Adamowski, J.F.; Liu, C.F.; Zhou, J.J.; Zhu, G.F.; Dong, X.G.; Gao, J.J.; Feng, Q. Which slope aspect and gradient provides the best afforestation-driven soil carbon sequestration on the China's Loess Plateau. *Ecol. Eng.* **2020**, *147*, 105782. [[CrossRef](#)]
25. Liu, S.L.; Dong, Y.H.; Cheng, F.Y.; Yin, Y.J.; Zhang, Y.Q. Variation of soil organic carbon and land use in a dry valley in Sichuan province, Southwestern China. *Ecol. Eng.* **2016**, *95*, 501–504. [[CrossRef](#)]
26. Huang, X.F.; Zhou, Y.C.; Zhang, Z.M. Characteristics and Affecting factors of Soil Organic Carbon Under land Uses: A Case Study in Houzhai River Basin. *J. Nat. Resour.* **2018**, *33*, 1056–1067.
27. Wang, X.F.; Huang, X.F.; Hu, J.W.; Zhang, Z.M. The soil organic carbon density spatial heterogeneity and its impact factors under different karst landforms. *Int. J. Glob. Warm.* **2020**, *22*, 174–195. [[CrossRef](#)]
28. Zhang, Y.; Shi, X.Z.; Zhao, Y.C.; Yu, D.S.; Wang, H.J.; Sun, W.X. Estimates and Affecting Factors of Soil Organic Carbon Storage in Yunnan- Guizhou-Guangxi Region of China. *Environ. Sci.* **2008**, *29*, 2314–2319.
29. Zhang, X.B.; Wang, S.J.; He, X.B.; Wang, Y.C.; Wen, A.B. A preliminary discussion on the rocky desertification classification for slope land in karst mountain areas of southwest China. *Earth Environ.* **2007**, *35*, 188–192.
30. Fisher, R.A. *Statistical Methods and Scientific Inference*; Oliver and Boyd: London, UK, 1956.
31. Haining, R. *Spatial Data Analysis: Theory and Practice*; Cambridge University Press: Cambridge, UK, 2010.
32. Hedley, C.B.; Payton, I.J.; Lynn, I.H.; Carrick, S.T.; Webb, T.H.; Mcneill, S. Random sampling of stony and non-stony soils for testing a national soil carbon monitoring system. *Soil Res.* **2012**, *50*, 18–29. [[CrossRef](#)]
33. Zhang, Z.M.; Zhou, Y.C.; Wang, S.J.; Huang, X.F. Soil organic carbon density spatial distribution and influencing factors in a karst mountainous basin. *Pol. J. Environ.* **2017**, *26*, 2363–2374. [[CrossRef](#)]
34. Wu, H.B.; Guo, Z.T.; Peng, C.H. Distribution and storage of soil organic carbon in China. *Glob. Biogeochem. Cycles* **2003**, *17*, 1048. [[CrossRef](#)]
35. Li, Z.P.; Han, F.X.; Su, Y.; Zhang, T.L.; Sun, B.; Monts, D.L.; Plodinec, J. Assessment of soil organic and carbonate carbon storage in China. *Geoderma* **2007**, *138*, 119–126. [[CrossRef](#)]
36. Wang, X.G.; Zhu, B.; Hua, K.K.; Luo, Y.; Zhang, J.; Zhang, A.B. Assessment of soil organic carbon stock in the upper Yangtze River Basin. *J. Mt. Sci.* **2013**, *10*, 866–872. [[CrossRef](#)]
37. Nelson, D.W.; Sommers, L.E. Total carbon, organic carbon, and organic matter. In *Methods of Soil Analysis, Agronomy*, 2nd ed.; Page, A.L., Miller, R.H., Keeney, D.R., Eds.; ASA and SSSA: Madison, WI, USA, 1982; pp. 539–577.
38. Wang, Z.P.; Han, X.G.; Li, L.H. Effects of grassland conversion to croplands on soil organic carbon in the temperate Inner Mongolia. *J. Environ. Manag.* **2008**, *86*, 529–534. [[CrossRef](#)] [[PubMed](#)]

39. Wang, Y.G.; Li, Y.; Ye, X.H.; Chu, Y.; Wang, X.P. Profile storage of organic/inorganic carbon in soil: From forest to desert. *Sci. Total Environ.* **2010**, *408*, 1925–1931. [[CrossRef](#)]
40. Dong, Y.Q.; Chen, Y.; Chen, Y.; Chen, D. Study on the Determination of Soil organic Carbon by Potassium Dichromate-Dryer Heating Methods. *J. Chang. Univ. Nat. Sci. Ed.* **2019**, *31*, 15–20.
41. Zhang, W.; Wang, K.L.; Chen, H.S.; He, X.Y.; Zhang, J.G. Ancillary information improves kriging on soil organic carbon data for a typical karst peak cluster depression landscape. *J. Sci. Food Agric.* **2012**, *92*, 1094–1102. [[CrossRef](#)]
42. Yuan, D.X. Carbon cycle in earth system and its effects on environment and resources. *Quat. Sci.* **2001**, *21*, 223–232.
43. Hu, L.N.; Su, Y.R.; He, X.Y.; Wu, J.S.; Zheng, H.; Li, Y.; Wang, A.H. Response of soil organic carbon mineralization in typical Karst soils following the addition of  $^{14}\text{C}$ -labeled rice straw and  $\text{CaCO}_3$ . *J. Sci. Food Agric.* **2012**, *92*, 1112–1118. [[CrossRef](#)]
44. Bai, Y.X.; Sheng, M.Y.; Hu, Q.J.; Zhao, C.; Wu, J.; Zhang, M.S. Effects of land use change on soil organic carbon and its components in karst rocky desertification of southwest China. *Chin. J. Appl. Ecol.* **2020**, *31*, 1607–1616.
45. Wang, S.Q.; Zhou, C.H.; Li, K.R.; Zhu, S.L.; Huang, F.H. Analysis on Spatial Distribution Characteristics of Soil Organic Carbon Reservoir in China. *Acta Geogr. Sin.* **2000**, *55*, 533–544.
46. Mi, N.; Wang, S.Q.; Liu, J.Y.; Yu, G.R.; Zhang, W.J.; Jobbágy, E. Soil inorganic carbon storage pattern in China. *Glob. Change Biol.* **2008**, *14*, 2380–2387. [[CrossRef](#)]
47. Subramanian, B.; Zhou, W.J.; Ji, H.L.; Grace, J.; Bai, X.L.; Song, Q.H.; Liu, Y.T.; Sha, L.Q.; Fei, X.H.; Zhang, X.; et al. Environmental and management controls of soil carbon storage in grasslands of southwestern China. *J. Environ. Manag.* **2020**, *254*, 109810. [[CrossRef](#)] [[PubMed](#)]